Journal of Digital Imaging

Radon-Domain Detection of the Nipple and the Pectoral Muscle in Mammograms

S. K. Kinoshita,[1,2] P. M. Azevedo-Marques,[1] R. R. Pereira Jr,[1] J. A. H. Rodrigues,[1] and R. M. Rangayyan[3,4]

In this paper, methods are presented for automatic detection of the nipple and the pectoral muscle edge in mammograms via image processing in the Radon domain. Radon-domain information was used for the detection of straight-line candidates with high gradient. The longest straight-line candidate was used to identify the pectoral muscle edge. The nipple was detected as the convergence point of breast tissue components, indicated by the largest response in the Radon domain. Percentages of false-positive (FP) and false-negative (FN) areas were determined by comparing the areas of the pectoral muscle regions delimited manually by a radiologist and by the proposed method applied to 540 mediolateral-oblique (MLO) mammographic images. The average FP and FN were 8.99% and 9.13%, respectively. In the detection of the nipple, an average error of 7.4 mm was obtained with reference to the nipple as identified by a radiologist on 1,080 mammographic images (540 MLO and 540 craniocaudal views).

KEY WORDS: Digital mammography, nipple detection, pectoral muscle detection, radon transform, image processing

INTRODUCTION

Computer-aided Diagnosis (CAD) of Breast Cancer

Mammograms are the method of choice for screening asymptomatic women for early detection of breast cancer. Such screening will necessarily generate a large number of mammograms, which must be viewed and interpreted by a limited number of expert radiologists.[5] Computer-aided diagnosis (CAD) is being used to obtain a second opinion in the analysis of mammograms and could serve to reduce the workload on radiologists.[5,16] CAD systems are used to identify suspicious lesions (calcifications, masses, and distortion of parenchymal tissue) and to quantify the density of the breast tissue. To accomplish these goals, a region of interest (ROI) may be extracted from the given mammogram, and/or the entire breast region may be analyzed.[9,11,12,29,30] In some methods, a bilateral comparison of mammograms is performed to detect asymmetry.[6] In all these cases, it is necessary to segment the breast area in the mammogram to identify ROIs. When mediolateral-oblique (MLO) mammograms are used, an additional step to segment the pectoral muscle is desirable because this region appears at approximately the same density as the dense tissues of interest in the image of the breast. Therefore, the

[1]*From the Image Science and Medical Physics Center, Internal Medicine Department, Faculty of Medicine of Ribeirão Preto, University of São Paulo, Avenida dos Bandeirantes, 3900, 14048-900, Ribeirão Preto, São Paulo Brazil.*

[2]*From the Department of Electrical Engineering, University of São Paulo, Avenida do Trabalhador Sancarlense 400, 13560-250, São Carlos, São Paulo, Brazil.*

[3]*From the Department of Electrical and Computer Engineering, Schulich School of Engineering, and Department of Radiology, University of Calgary, Calgary, Alberta T2N 1N4, Canada.*

[4]*From the Department of Radiology, University of Calgary, Calgary, Alberta T2N 1N4, Canada.*

Correspondence to: P. M. Azevedo-Marques, Image Science and Medical Physics Center, Internal Medicine Department, Faculty of Medicine of Ribeirão Preto, University of São Paulo, Avenida dos Bandeirantes, 3900, 14048-900, Ribeirão Preto, São Paulo Brazil; tel: +55-16-36022647; fax: +55-16-36022648; e-mail: pmarques@fmrp.usp.br

Online publication 11 April 2007
doi: 10.1007/s10278-007-9035-6

breast tissue must be isolated from the pectoral muscle and background.[7] The straight line that separates the region of the pectoral muscle from the breast is important also in automatic alignment of mammograms for bilateral analysis and detection of asymmetry (due to masses, architectural distortion, etc.) via the subtraction of left and right mammograms.[15,30] Karssemeijer[11] used the Hough transform and a set of threshold values applied to the accumulator cells to detect a straight-line approximation of the edge of the pectoral muscle. The Radon transform has also been used to locate linear structures in images.[19,27] In this paper, we describe a Radon-domain method for automatic detection of a straight line approximating the edge of the pectoral muscle.

Furthermore, automatic detection of the nipple would be useful in the alignment and registration of mammograms.[5,15] Anatomically, the nipple is the only landmark on the breast region (skin–air interface). Glandular structures (lobules, ducts, etc.) converge to the nipple. Radiologists use the nipple as a reference to compare the corresponding regions of the right and left breasts to detect relative anomalies.[5] We use the characteristics mentioned above to detect the nipple, employing the Radon transform to locate linear structures in a given mammographic image.

The images acquired for the study were observed to be noisy. The preprocessing step implemented for image quality improvement is also described in the following sections.

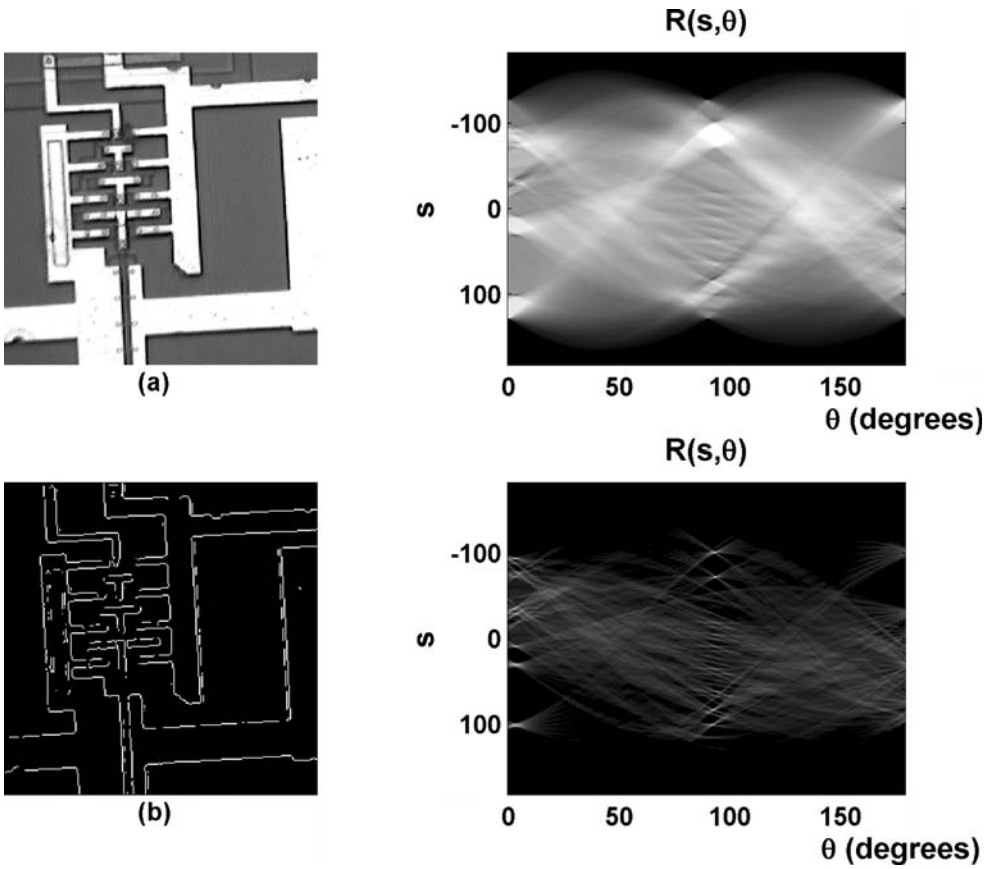

Fig 1. A simple test image and its Radon transform (image obtained from http://www.mathworks.com/company/newsletters/news_notes/images/circuit1.gif). The Radon domain displays large values at ray angles (θ) and positions (s) that correspond to strong linear features in the image. (a) Original gray-level image and the corresponding Radon transform, and (b) binary image representing the edges in the image and the corresponding Radon transform.

The Radon Transform

The Radon transform of an image is the projection (integral) of the image at a given angle.[19] Each point in the Radon domain (s, θ) corresponds to the integration of the image along a straight line (ray) in the spatial domain (x, y) of the image. The intensities of strong peaks in the Radon domain correspond to the locations (direction θ and distance s) of high intensities in the original gray-level image or to straight lines in a binary image (see Fig. 1). The Radon transform forms the basis for the representation of images by their projections (ray integrals), as well as image reconstruction from projections and computed tomography.[20,23] Several algorithms for image processing and analysis may be applied advantageously in the Radon domain, for applications such as the detection of edges,[27] analysis of oriented patterns,[19] analysis of spicules and architectural distortion in mammograms,[25] and deconvolution via the complex cepstrum.[13,14]

We apply the Radon transform to two types of images: (1) binary images for the detection of straight lines, leading to the edge of the pectoral

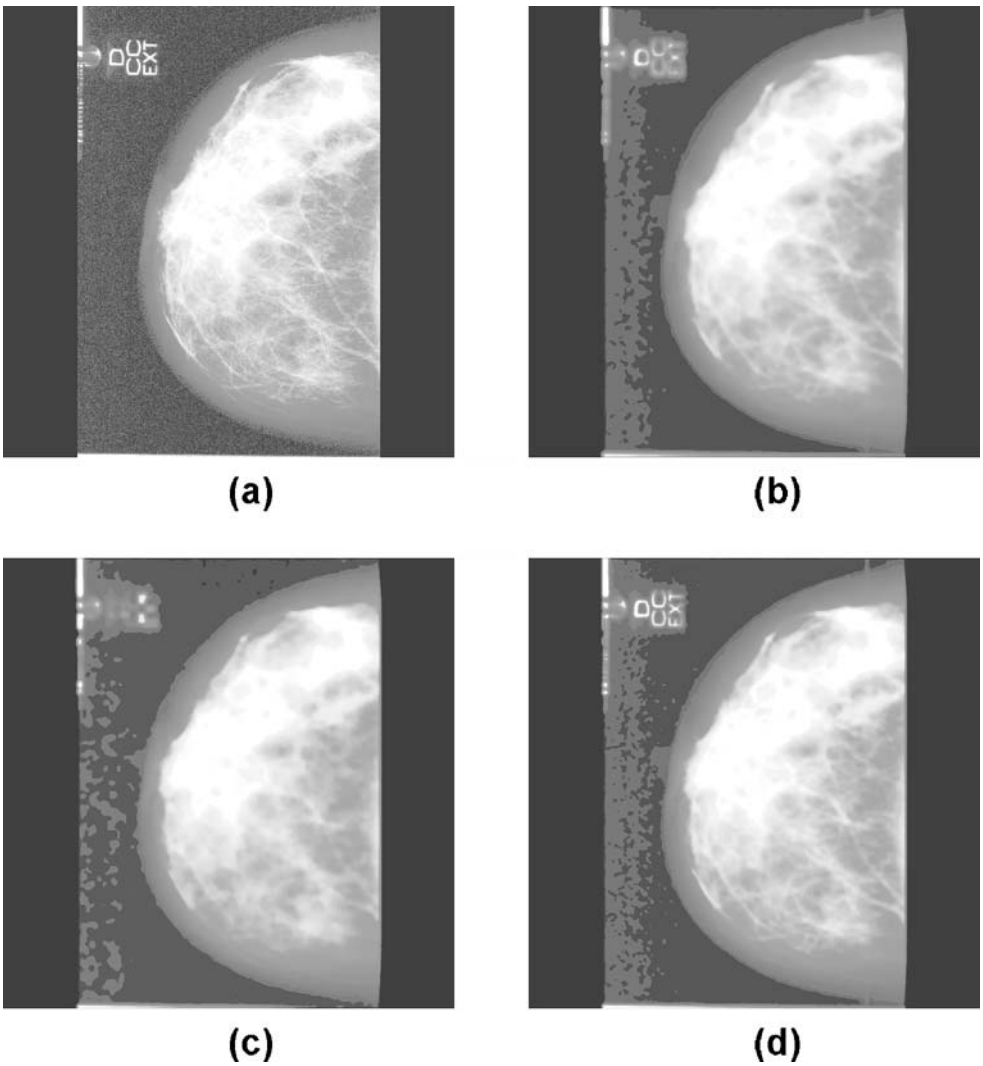

Fig 2. Examples of results of filtering a noisy mammogram with anisotropic diffusion using different prefiltering methods: (a) original noisy image; (b) prefiltering with a Gaussian filter (signal-to-noise ratio = 19.7 dB); (c) prefiltering with the morphological open–close filter (signal-to-noise ratio = 19.0 dB); (d) prefiltering with the Wiener filter (signal-to-noise ratio = 22.3dB).

muscle, and (2) gray-level images for the detection of maximum-intensity peaks for selected projections at specific positions s and directions θ, to detect the nipple.

METHODS

Image Data set

A set of 1,080 mammograms was prepared, including 270 pairs (left–right) of craniocaudal (CC) views and 270 pairs of MLO views from the Medical Center of the Faculty of Medicine, University of São Paulo, Ribeirão Preto, São Paulo, Brazil. The films were digitized using a Vidar DiagnosticPro scanner with a resolution of 300 dpi (pixel size of 85 μm) and 12 bits per pixel.

Films of two sizes were included in the data set: 24×30 and 18×24 cm. The digitized image matrices were of size $2{,}835 \times 3{,}543$ and $2{,}126 \times 2{,}835$ pixels, respectively. The images were cropped to remove patient and imaging markers. To reduce computational requirements,

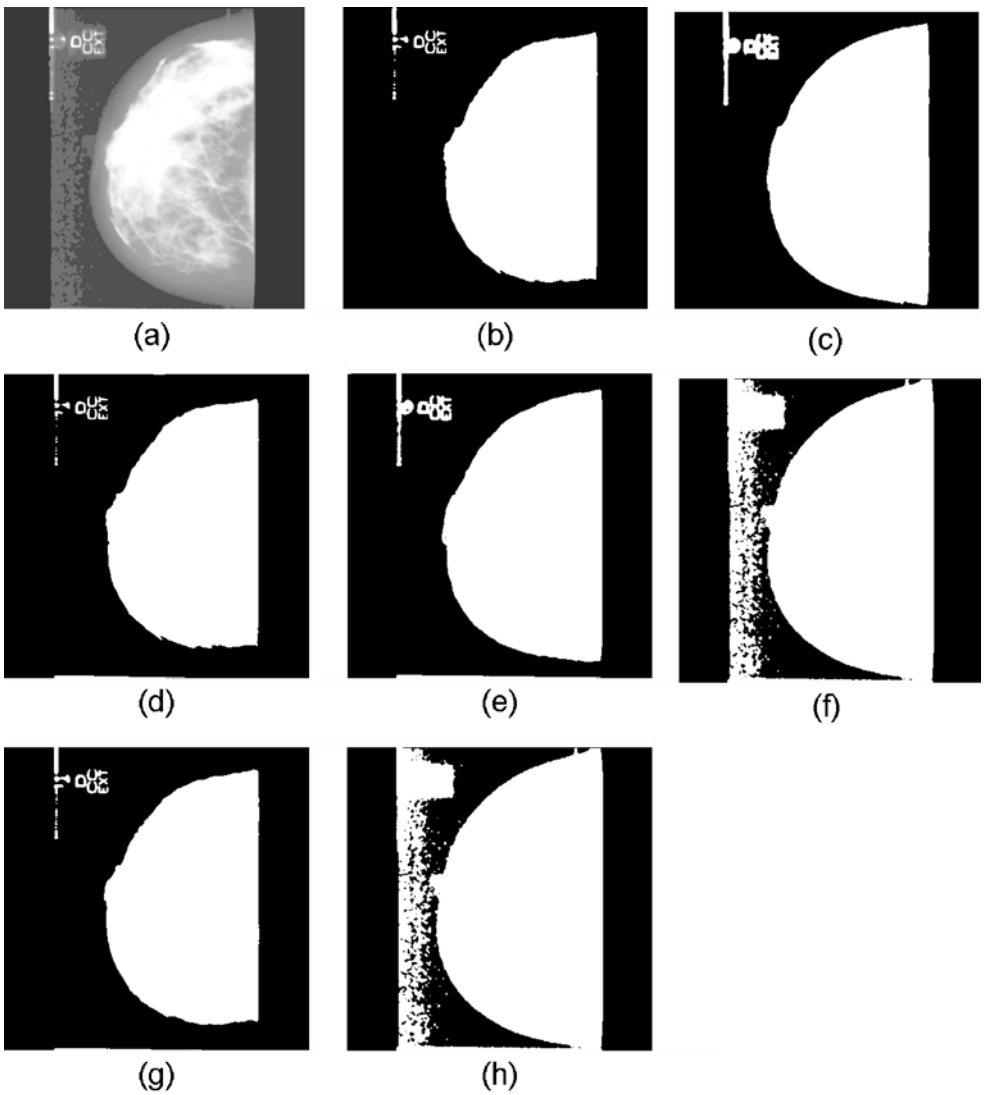

Fig 3. Examples of the results of the segmentation of the effective breast area: (a) original image; (b) maximum-entropy principle; (c) moment-preserving method; (d) Otsu's method; (e) method of Ridler and Carvard; (f) method based on the spatial gray-level dependence matrix (SGLD); (g, h) maximum and minimum threshold of the method of Reddi et al.

the images were down-sampled, without loss of significant information, to matrices of size $1{,}024 \times 1{,}024$ pixels, with an effective resolution of 279 and 223 μm for the two film sizes mentioned above. The pixel sizes were taken into account in the determination of measures of error, in millimeters, in the positions of the nipple and the pectoral muscle edge detected.

Preprocessing of Mammograms

Perona and Malik[18] developed the method of anisotropic diffusion for the removal of noise in images; the objective of this method is to smooth a local image region while preserving its edges. However, the removal of small-scale artifacts with high contrast is difficult. To alleviate this problem, the image may be filtered before the application of the anisotropic diffusion equation. Catté et al[3,4] used a Gaussian filter before the application of anisotropic diffusion. The purpose of prefiltering was to remove small features with high contrast while preserving the significant edges in the image. Segall and Acton[26] applied the morphological open-close filter with adjustment of the size of the structuring element, so as

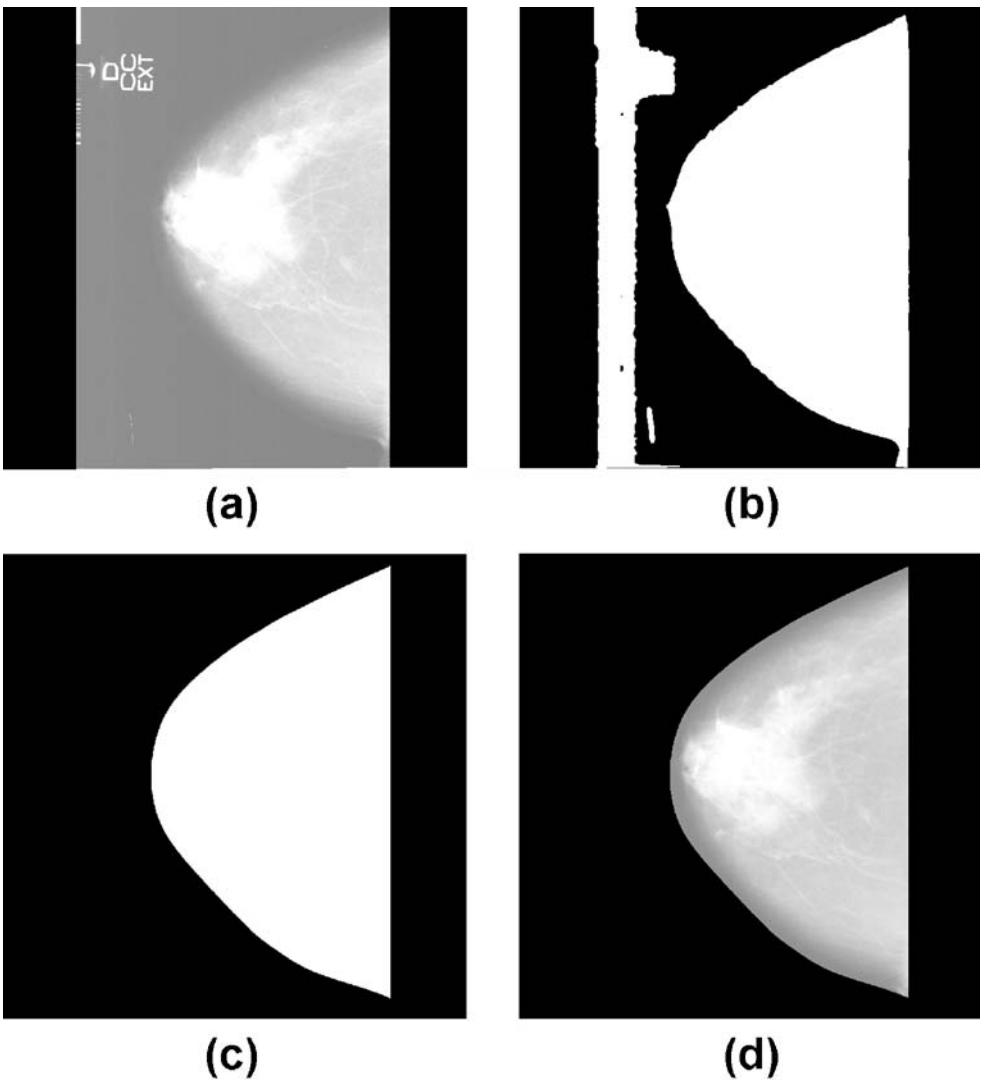

Fig 4. Example of the segmentation of the effective breast region: (a) original image; (b) the segmented image; (c) the image after spurious objects were removed from the background and the edge was smoothed; (d) the final result of segmentation.

to smooth objects smaller than the structuring element while maintaining edge structure and location. However, these methods were not adequate for the recovery of the edge elements degraded by high levels of noise. As an alternative, the Wiener filter was chosen in this work because of its ability to restore degraded images.[8] Figure 2 presents a comparative illustration of the results of application of anisotropic diffusion with the Gaussian, morphological open–close, and Wiener filters to a noisy mammogram.

Segmentation of the Breast Region and Edge Detection

After filtering to remove noise, segmentation of the breast region was performed as follows. Several thresholding methods were applied to each image, including the maximum-entropy principle,[10] moment-preserving method,[28] Otsu's method,[17] the method of Ridler and Calvard,[22] the method of Reddi et al,[21] and a method based upon the spatial gray-level dependence (SGLD) ma-

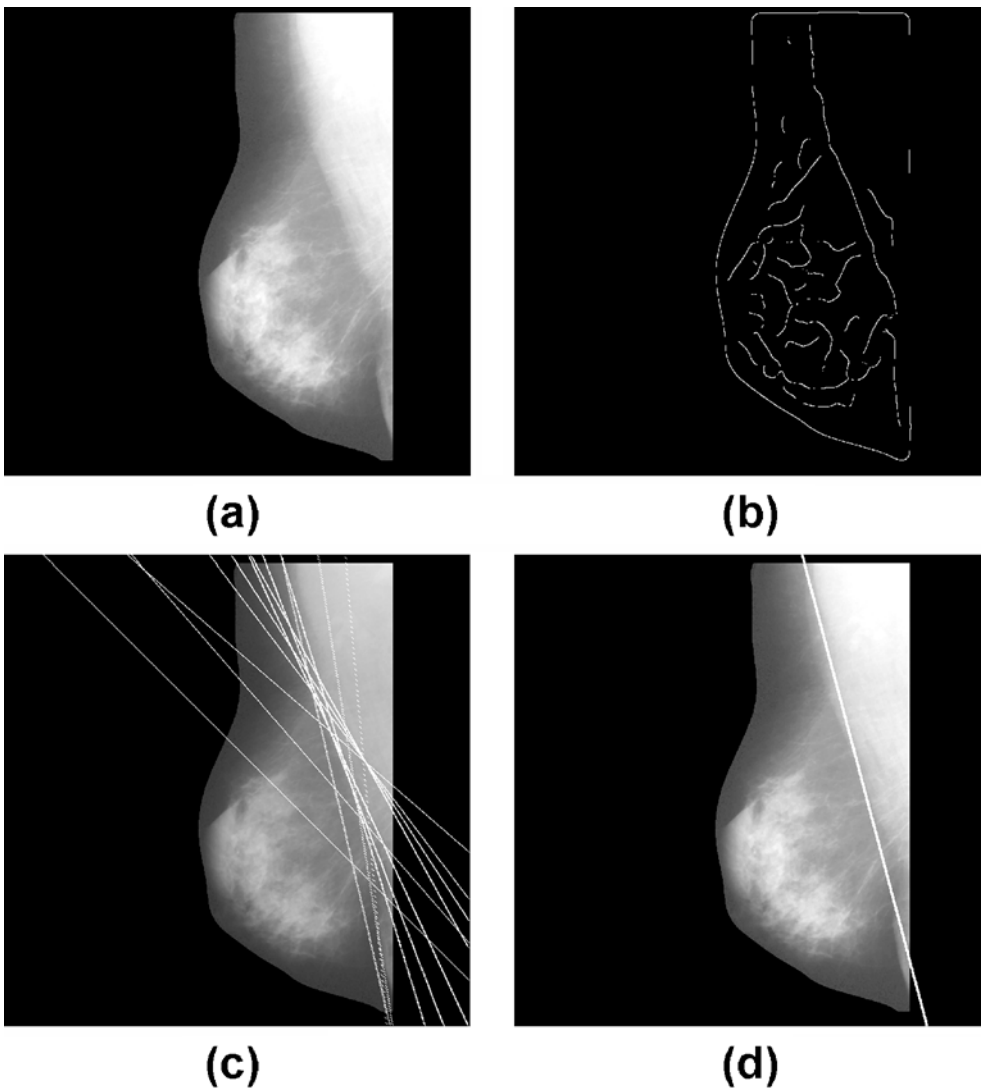

Fig 5. An example of the detection of the edge of the pectoral muscle, approximated by a straight line: (a) original image; (b) the edge image obtained using the Canny filter; (c) detection of straight-line candidates by the Radon transform; (d) selection of the pectoral muscle edge by the criteria adopted. (See the text for details.)

trix.[24] The best result among the above was selected for each image by one of the radiologists involved in the study. Figure 3 shows a mammogram and the result of segmentation using each of the thresholding methods mentioned above. Morphological opening and closing operations were used to remove small artifacts in the image and to smooth the contour of the breast region. In addition, B-spline interpolation was applied using 32-pixel control-point intervals to obtain the final contour of the breast region.

To obtain the effective breast region from a given mammogram, the result of segmentation as above was used in the form of a mask and multiplied with the original mammogram. Figure 4 shows the results of the various steps in the segmentation of a mammogram.

Detection of the Pectoral Muscle

The pectoral muscle region (in MLO mammograms) has a predominantly high density that

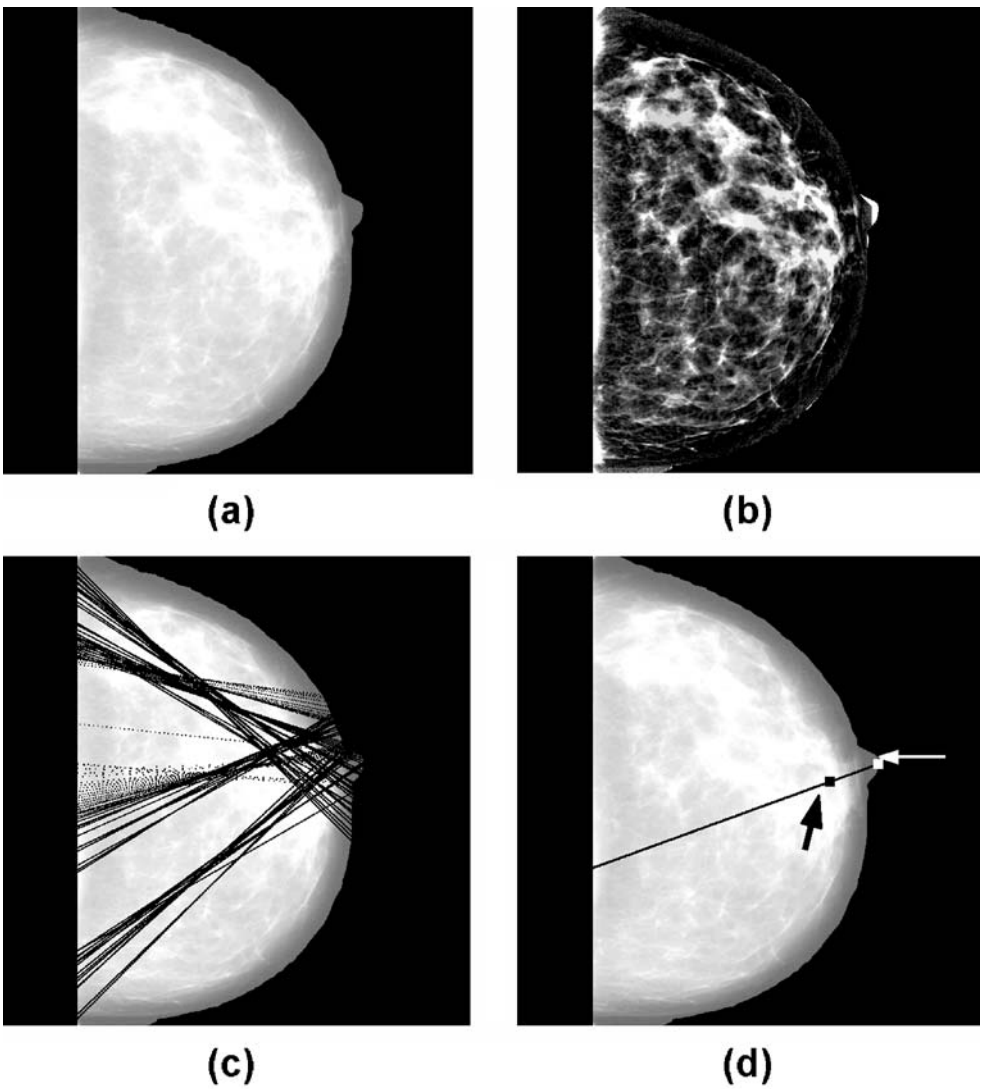

Fig 6. Illustration of the sequence of operations for the detection of the nipple: (a) original image (left breast, CC view); (b) result of the top-hat filter; (c) straight lines corresponding to the maximum values of the Radon transform in the directions $-45 \leq \theta \leq -135$ degrees, where θ is the angle of the Radon transform (projection); (d) the white point (white arrow) indicates the nipple position detected and the black point (black arrow) represents the point of convergence. (See the text for details.)

could interfere with the analysis of mammograms: prior detection and removal of this region could lead to improved results with CAD algorithms.[7] The high density of the pectoral muscle results in a strong edge that can be approximated by a straight line. We propose to use the Radon transform[19,20] to detect the edge of the pectoral muscle region, as follows.

The Canny filter,[2] based on a Gaussian profile and gradient estimation, was applied for edge detection. The Radon transform of the edge image was computed. To identify the pectoral muscle region, a straight line was used to approximate the separation between the breast and pectoral muscle tissues. Straight-line candidates were detected by applying the Radon transform in the angle interval between 5° and 50° for right breast images, and between −5° and −50° for left breast images. The criteria of maximum intensity in the Radon domain and localization close to the thoracic wall were applied to detect a straight line to represent the edge of the pectoral muscle region. Figure 5 presents an example illustrating the detection of the straight-line approximation to the pectoral muscle edge in a mammogram.

Detection of the Nipple

To develop a process for automatic detection of the position of the nipple in a mammographic image, the following features of breast anatomy were considered: 1) the nipple is located on the breast surface; 2) glandular tissues contain structures (lobes, ducts, etc.) that converge toward the nipple and appear as bright (radio-opaque) regions, whereas adipose and low-density tissues appear as darker regions in mammograms.

The morphological top-hat filter was applied to the mammogram to enhance the breast structures converging toward the nipple.[8] The top-hat filter includes a closing operation in accordance with a structuring element, followed by subtraction of the filtered image from the original. A disk-shaped structuring element with a radius of 50 pixels was used. The filter enhances selected features based on the size and shape of the structuring element specified, and also darkens the background elements (see Fig. 6). When processing MLO views, the pectoral muscle region was removed from the image before the application of the top-hat filter.

The Radon transform was applied to the result of the top-hat filter as above. For MLO views, the angle intervals used were $45° + \alpha \leq \theta \leq 135° + \alpha$ for right breast images and $-45° - \alpha \leq \theta \leq -135° - \alpha$ for left breast images, where α is the direction of the pectoral muscle edge (straight-line approximation) and θ is the angle in the Radon domain. For CC views, the angle intervals were $45° \leq \theta \leq 135°$ and $-45° \leq \theta \leq -135°$ for right and left breast images, respectively. The point in the mammogram containing the highest number of converging lines is expected to be proximal to the nipple (see Fig. 6c). Given that the nipple is located on the breast surface (breast edge or boundary in the mammogram), its position was located as follows: The Radon transform of the gray-level mammogram (before the application of the top-hat filter) was searched to locate the ray with the maximum intensity that crosses the point of convergence; this straight line was extended to the breast boundary to detect the nipple (see Fig. 6d).

RESULTS AND DISCUSSION

The evaluation of the methods for filtering and segmentation of mammograms was performed by

Table 1. Analysis of Error in the Detection of the Pectoral Muscle: Mean and Standard Deviation Values of False-Positive (FP) and False-Negative (FN) Areas, the Hausdorff Distance, and the Numbers of Images Where the Results are Considered to be Accurate (FP and FN ≤ 5%), Acceptable (5% < FP and FN ≤ 15%), and not Acceptable (FP and FN > 15%)

False-Positive and False-Negative Areas	Values	Number of Images
FP (%) ($\mu \pm \sigma$)	8.99 ± 38.72	
FN (%) ($\mu \pm \sigma$)	9.13 ± 11.87	
# Images with (FP and FN) < 5%	156 (28.9%)	
# Images with 5% < (FP and FN) < 15%	220 (40.7%)	
# Images with (FP and FN) > 15%	164 (30.4%)	540 (100%)
Hausdorff distance (mm) ($\mu \pm \sigma$)	12.45 ± 22.96	

The errors are with respect to the pectoral muscle edge identified manually by a radiologist.

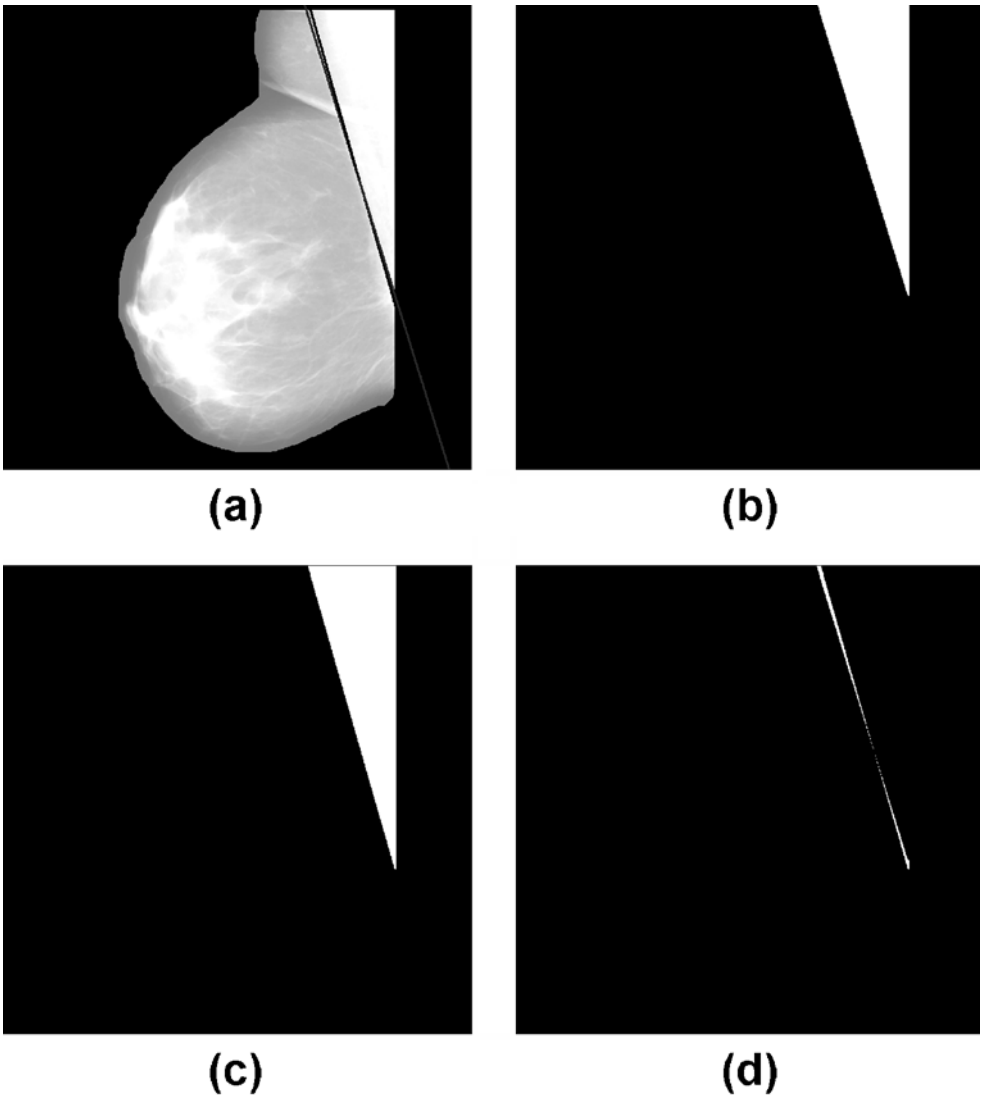

Fig 7. Example of an accurate detection of the pectoral muscle region: (a) Image showing the straight line manually detected by a radiologist (in black) and automatically detected by the proposed method (in gray); (b) image of the pectoral muscle region segmented based on the manually detected straight line; (c) image of the pectoral muscle region segmented based on the straight line detected by the proposed methods; (d) image with FP and FN regions obtained from the difference between the images in (b) and (c). Quantitative error values are FP = 1.2%, FN = 3.0%, FP and FN combined = 4.2%, and Hausdorff distance = 4.47 mm.

a radiologist. The acceptance grade was determined in relation to the amount of suppressed or increased breast tissues apparent in the image. The results indicated that, for CC images, seven (1.3%) images were not acceptable, 156 (28.9%) were acceptable, and 377 (69.8%) were accurate. For MLO views, the results indicated that 21 (3.9%) images were not acceptable, 154 (28.5%) were acceptable, and 365 (67.6%) were accurate. Here, "accurate" means that the segmentation was almost perfect; "acceptable" means that some breast tissue was excluded or some non-breast tissue was included in the segmented result, but the final image is acceptable for diagnosis; and "not acceptable" means that the final image is not good for diagnosis.

The method for the detection of the pectoral muscle edge was applied to 540 MLO mammographic images. To evaluate the result of automatic detection of the pectoral muscle edge, a radiologist specialized in mammography independently determined the pectoral muscle edge

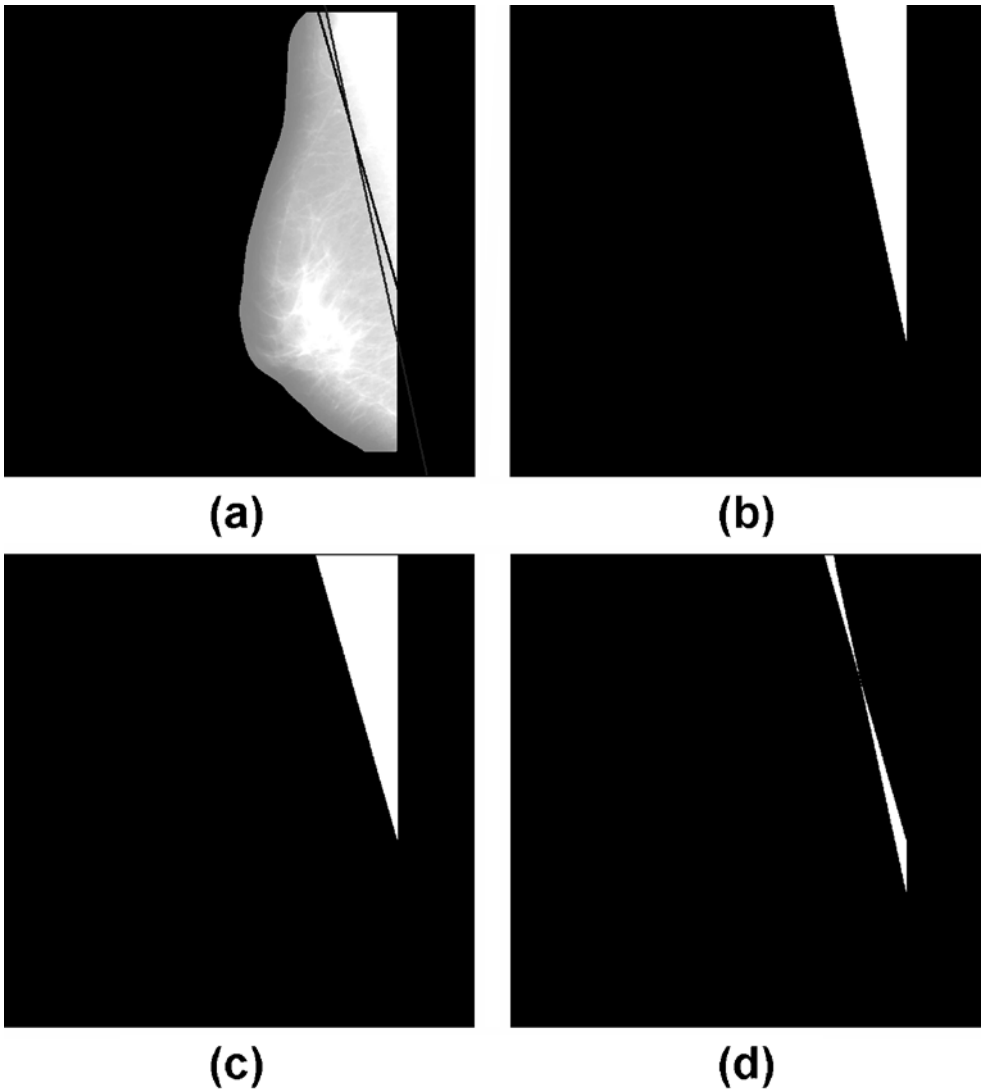

Fig 8. Example of an acceptable detection of the pectoral muscle region: (a) Image showing the straight line manually detected by a radiologist (in black) and automatically detected by the proposed method (in gray); (b) image of the pectoral muscle region segmented based on the manually detected straight line; (c) image of the pectoral muscle region segmented based on the straight line detected by the proposed methods; (d) image with FP and FN regions obtained from the difference between the images in (b) and (c). Quantitative error values are FP = 4.2%, FN = 9.9%, FP and FN combined = 14.1%, and Hausdorff distance = 5.31 mm.

(approximated by a straight line) by visual analysis. The automatically detected edges were evaluated by using the percentages of false-positive (FP) and false-negative (FN) pixels normalized with reference to the corresponding numbers of pixels in the pectoral muscle region manually delimited by the radiologist.[7] Of the 540 images processed, the results were considered to be accurate (FP and FN $\leq$ 5%) for 156 images (28.9%); acceptable (5% $<$ FP and FN $\leq$ 15%) for 220 images (40.7%); and not acceptable (FP and FN $>$ 15%) for 164 images (30.4%). The mean and standard deviation values of the FP and FN rates as well as the Hausdorff distance (see the Appendix) between the automatically detected and manually delimited pectoral muscle edges were computed and are presented in Table 1.

Figures 7 and 8 illustrate two examples of pectoral muscle edge detection considered to be accurate (FP = 1.2%, FN = 3.0%, FP and FN

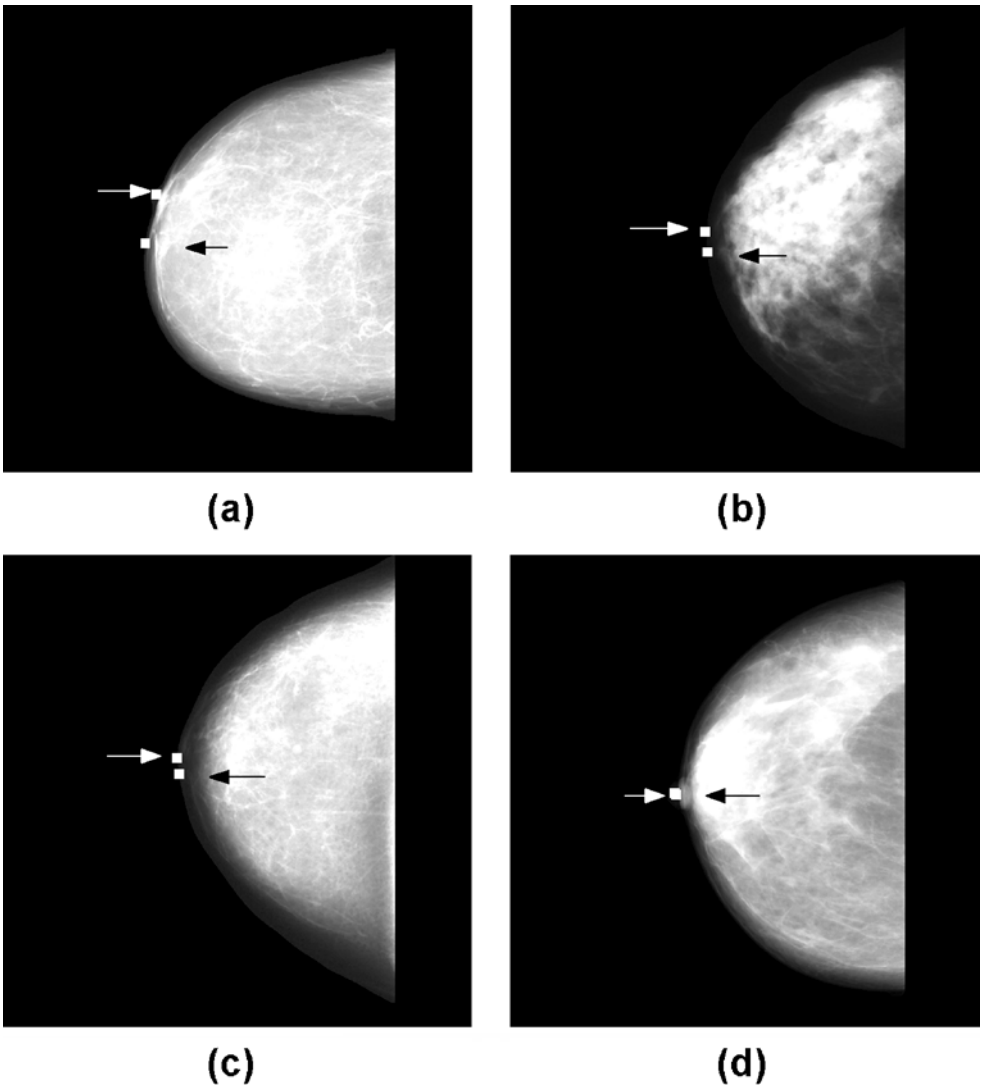

Fig 9. Examples of detection of the nipple: (a) error = 24.1 mm; (b) error = 9.8 mm; (c) error = 7.8 mm; (d) error = 1.0 mm. Two points are shown on each mammogram, corresponding to the nipple positions detected automatically by the proposed method (black arrow) and manually by a radiologist (white arrow).

Table 2. Distribution of Images by the Range of the Absolute Error in Millimeters in the Detection of the Nipple, as Compared to the Same Identified by a Radiologist

	≤5 mm	5 to 10 mm	10 to 15 mm	15 to 20 mm	>20 mm	Total
MLO right	146	52	27	16	29	270
MLO left	114	80	27	20	29	270
CC right	157	67	22	14	10	270
CC left	168	72	14	7	9	270
Total	585	271	90	57	77	1080

combined = 4.2%) and acceptable (FP = 4.2%, FN = 9.9%, FP and FN combined = 14.1%), respectively.

The results of the method for the detection of the edge of the pectoral muscle show that the performance is related to the appearance of the edge of the pectoral muscle in the mammogram. Of the 376 images with results considered to be accurate and acceptable, 80.0% (301/376) had pectoral muscles with straight edges, 10.9% (41/376) had considerably curved edges, and 9.1% (34/376) had poorly defined edges with low contrast. Of the 164 images with results considered to be unacceptable, 14.0% (23/164) had pectoral muscles with straight edges, 37.2% (61/164) had been considerably curved edges, and 48.8% (80/164) had poorly defined edges. Therefore, the method had better performance with images with straight-line edges and worse performance with other types of edges of the pectoral muscle region.

The method for the detection of the nipple was applied to 540 MLO and 540 CC mammographic images. Figure 9 shows four mammograms with different levels of error in the detection of the nipple. The absolute error between the detected position and that identified by the radiologist was, on the average, 7.4 mm over the 1,080 images processed. Table 2 shows the distribution of images by the range of error in millimeters. Out of the 1,080 images processed, the results were considered to be accurate (error $\leq$5 mm) in 585 images (54.2%); acceptable (5 mm $<$ error $\leq$ 10 mm) in 271 images (25.1%); and not acceptable (error >10 mm) in 224 images (20.7%).

The results obtained show that the performance of the method for detection of the nipple is related to the quality of the image of the breast region after the initial preprocessing step. Of the 224 images with results considered to be not acceptable, 88.4% (198/224) images had been considered to be not acceptable or acceptable, and 11.6% (26/224) had been considered to be accurate after the initial preprocessing step.

CONCLUSION

We have presented techniques for the detection of a straight-line approximation to the edge of the pectoral muscle and detection of the nipple in noisy mammograms, by the application of image processing and pattern recognition techniques in the Radon domain. The Radon transform offers readily identifiable and useful information related to oriented patterns in mammograms that can, in turn, be related to the edge of the pectoral muscle and the parenchymal patterns that converge toward the nipple.

The results of evaluation of the proposed methods with a large number of mammograms indicate the success of the methods in the detection of important features in noisy mammograms that could be useful in CAD algorithms for the analysis of mammograms and diagnosis of breast cancer.

ACKNOWLEDGMENT

We thank the radiologists and faculty members of the Medical Center of the Faculty of Medicine, University of São Paulo, Ribeirão Preto, Brazil, for providing the mammograms used in this work. We thank the State of São Paulo Research Foundation (FAPESP); the National Council for Scientific and Technological Development (CNPq); the Foundation to Aid Teaching, Research, and Patient Care of the Clinical Hospital of Ribeirão Preto (FAEPA/HCRP); and the Catalyst Program of Research Services of the University of Calgary for financial support.

APPENDIX

Hausdorff Distance

Hausdorff distance[1] is the maximum distance of the points in a set to the corresponding nearest points in another set. Formally, the Hausdorff distance from set **A** to set **B** is a *maximin* function, defined as

$$\mathrm{h}(\mathrm{A},\mathrm{B}) = \max_{a\in A}\left\{\min_{b\in B}\{\mathbf{d}(\mathbf{a},\mathbf{b})\}\right\}$$

where, $\boldsymbol{a}$ and $\boldsymbol{b}$ are points of sets **A** and **B**, respectively, and $\boldsymbol{d}(\boldsymbol{a},\boldsymbol{b})$ is any metric between these points; for simplicity, we take $\boldsymbol{d}(\boldsymbol{a},\boldsymbol{b})$ as the Euclidian distance between $\boldsymbol{a}$ and $\boldsymbol{b}$.

REFERENCES

1. Belogay E, Cabrelli C, Molter U, Shonkwiler R: Calculating the Hausdorff distance between curves. Inf Process Lett 64:17–22, 1997

2. Canny J: A computational approach to edge detection. IEEE Trans Pattern Anal Mach Intell 8(6):679–698, 1986

3. Catté F, Lons PL, Morel JM, Coll T: Image selective smoothing and edge detection by nonlinear diffusion-I. SIAM J Numer Anal 29(1):182–193, 1992

4. Catté F, Lons PL, Morel JM, Coll T: Image selective smoothing and edge detection by nonlinear diffusion-II. SIAM J Numer Anal 29(1):845–866, 1992

5. Chandrasekhar R, Attikiouzel Y: A simple method for automatically locating the nipple on mammograms. IEEE Trans Med Imag 16(5):483–494, 1997

6. Ferrari RJ, Rangayyan RM, Desautels JEL, Borges RA, Frère AF: Analysis of asymmetry in mammograms via directional filtering with Gabor wavelets. IEEE Trans Med Imag 20(9):953–964, 2001

7. Ferrari RJ, Rangayyan RM, Desautels JEL, Borges RA, Frère AF: Automatic identification of pectoral muscle in mammograms. IEEE Trans Med Imag 23(2):232–245, 2004

8. Gonzalez RC, Woods RE: Digital image processing. Boston, MA: Addison Wesley Pub. Co. Inc, 1993

9. Hou Z, Giger ML, Wolverton DE, Zhong W: Computerized analysis of mammographic parenchymal patterns for breast cancer risk assessment: feature selection. Med Phys 27(1):4–12, 2000

10. Kapur JN, Sahoo PK, Wong AKC: A new method for grey-level picture thresholding using the entropy of the histogram. Comput Vis Graph Image Process 29:273–285, 1985

11. Karssemeijer N: Automated classification of parenchymal pattern in mammograms. Phys Med Biol 43:365–378, 1998

12. Kinoshita SK, Azevedo Marques PM, Frére AF, Marana HRC, Ferrari RJ, Villela RL: Comparative analysis of shape and texture features in classification of breast masses in digitized mammograms. In: Hanson KM Ed. Medical Imaging. Proceedings of SPIE 2000; 3979, pp 872–879

13. Martins ACG, Rangayyan RM: Texture element extraction via cepstral filtering in the Radon domain. IETE Journal of Research India. 48(3&4):143–150, 2002

14. Martins ACG, Rangayyan RM: Complex cepstral filtering of images and echo removal in the Radon domain. Pattern Recogn 30(11):1931–1938, 1997

15. Mendez AJ, Tahoces PG, Lado MJ, Souto M, Correa JL, Vidal JJ: Automatic detection of breast border and nipple in digital mammograms. Comput Methods Programs Biomed. 49:253–262, 1996

16. Nishikawa RM, Giger ML, Vyborny CJ, Bick U, Doi K, Schmidt RA: Prospective computer analysis of cancer missed on screening mammography. In: Yaffe MJ Ed. Proceedings of 5th International Workshop on Digital Mammography, Toronto, Canada, 2000, pp 493–498

17. Otsu N: A threshold selection method from grey-level histogram. IEEE Trans Syst Man Cybern 8:62–66, 1978

18. Perona P, Malik J: Scale-space and edge detection using anisotropic diffusion. IEEE Trans Pattern Anal Mach Intell 12(7):629–639, 1990

19. Rangayyan RM, Rolston WA: Directional image analysis with the Hough and Radon transforms. J Indian Inst Sci 78:3–16, 1998

20. Rangayyan RM: Biomedical Image Analysis. Boca Raton FL: CRC Press, 2005

21. Reddi SS, Rudin SF, Keshavan HR: An optimal multiple threshold scheme for image segmentation. IEEE Trans Syst Man Cybern 14:661–665, 1984

22. Ridler T, Carvard S: Picture thresholding using an iterative selection method. IEEE Trans Syst Man Cybern 8:630–632, 1978

23. Robb RA: X-ray computed tomography: an engineering synthesis of mulitscientific principles. CRC Crit Rev Biomed Eng 7:264–333, 1982

24. Sahoo PK, Soltani S, Wong AKC, Chen YC: A survey of thresholding techniques. Comput Vis Graph Image Process 41:233–260, 1988

25. Sampat MP, Whitman GJ, Markey MK, Bovik AC: Detection of spiculated lesions in mammograms. In Fitzpatrick M, Reinhardt JM Eds. Imaging Processing. Proceedings of SPIE Medical Imaging 2005. Vol. 5747, pp 26–37

26. Segall CA, Acton ST: Morphological anisotropic diffusion. IEEE International Conference on Image Processing, Santa Barbara, CA, October 26–29. 3:348–351, 1997

27. Srinivasa N, Ramakrishnan KR, Rajgopal K: Detection of edges from projections. IEEE Trans Med Imag 11(1):76–80, 1992

28. Tsai W: Moment-preserving thresholding: a new approach. Comput Vis Graph Image Process 29:377–393, 1985

29. Zhou C, Chan H-P, Petrick N, Helvie MA, Goodsitt MM, Sahiner B, Hadjiski LM: Computerized image analysis: estimation of breast density on mammograms. Med Phys 28(6):1056–1069, 2001

30. Yin FF, Giger ML, Doi K, Vyborny CJ, Schmidt RA: Computerized detection of masses in digital mammograms: analysis of bilateral subtraction images. Med Phys 18(5):955–963, 1994